Mechanism of dust removal by a standing wave electric curtain

SUN QiXia, YANG NingNing, CAI XiaoBing[*] & HU GengKai[*]

School of Aerospace Engineering, Beijing Institute of Technology, Beijing 100081, China

In this paper, the mechanisms of particle movement on an electric curtain are examined. Intermittent bursts in which particles leaping from a surface of an electric curtain are demonstrated both by numerical simulation and experimental observation. The hopping and surfing modes during particle removal are shown to depend on the particle electric charge and its initial position. The particles initially located on the top of electrode have a large electric charge tend to assume a hopping mode. Transverse movement of the particle initially located between the electrodes is analyzed, and the particle traps along the electric curtain surface are also observed.

The space above the moon surface is suffused with a massive amount of fine dust, and these dust particles are often electrically charged [1,2]. Under the low gravity, zero magnetic field and hard vacuum environment, these dust particles can float up several thousand meters [3,4]. The tiny dust particles are adhesive and can easily deposit and attach to exposed surfaces of a rover device, posing serious concerns for lunar surface exploration [5]. For example, the deposit of dust on solar panel can provoke a loss of power and impair 16% of power output in the first year as measured during the Survey 3 mission [6]. In addition, the dust can lead to imaging problem, false instrument readings and thermal control failure [7,8].

In order to mitigate the dust contamination, different techniques have been proposed for dust removal and prevention such as fluid jet, acoustic vibration, mechanical brushing and dynamic electric curtain [9,10]. However the environment on the moon surface and cost stringency limit most of the above techniques [10]. Instead, the electric cur-

tain (EC) technique, proposed by Tatom et al. [10], seems more promising, since it employs only a printed circuit layer of alternating parallel electrodes devoid of any mechanical component [11–14]. When the electrode is energized by an AC voltage, a strong dynamic electric field can be generated over the surface of the EC and the dust particles. These are then polarized, thus the dust leap away from the surface by dielectrophoresis forces and Coulomb forces. Figure 1 shows an electric curtain with dust covered and removed before and after power is loaded.

With an increasing interest in lunar or Mars explorations, the EC technique has attracted a growing interest in hope to confront the dust problem [15–21]. However, the EC technique is still far from being practical. Electric curtains should be designed optimally in order to meet energy and reliability requirement. The optimized design for structural and electrical parameters of EC depends on a clear understanding on particle removal mechanism. Machowski et al. [22] reported that the shape of electrodes has a significant influence on the performance of EC. They showed that rectangle electrodes are more efficient for dust removal compared to their circular and triangular counterparts. It is also
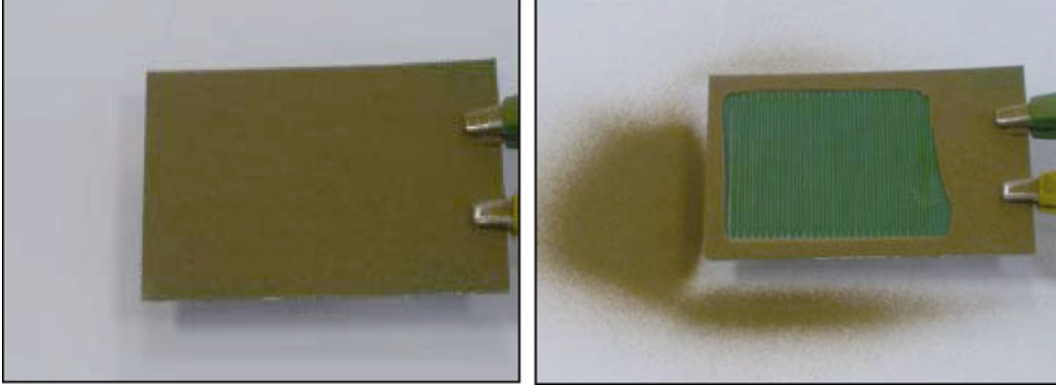
Figure 1 An electric curtain with dusts deposited and removed before and after energizing.

shown that particle size distribution [23], width of EC electrode [24] and shape of incident wave [25] all affect the dust removal efficiency.

However the particle leaping mechanism from an electric curtain for dust removal efficiency still needs more investigation. In this paper, we will analyze the mechanism of particle movement on a standing wave electric curtain both by numerical simulation and experimental observation. A computation method on motion of dust particles will be explained in sect. 1, and the detailed mechanisms during particle leaping process will be analyzed in sect. 2.

1 Particle dynamic simulation

In order to simulate the motion of particle loaded by an electric curtain, a two-dimensional model is proposed by using particle dynamic simulation method [26], which is shown in Figure 2. The parallel electrodes are etched on a dielectric board and then covered with an insulator layer of thickness h. The rectangular electrodes are of width a and thickness 0.032 μm, spanned with a spacing b. The voltage applied between the electrodes is denoted by U_0.

To simulate the motion of particles, we initially compute the electric field generated by the electric curtain, and then the force exerting on the particles. When the particles are
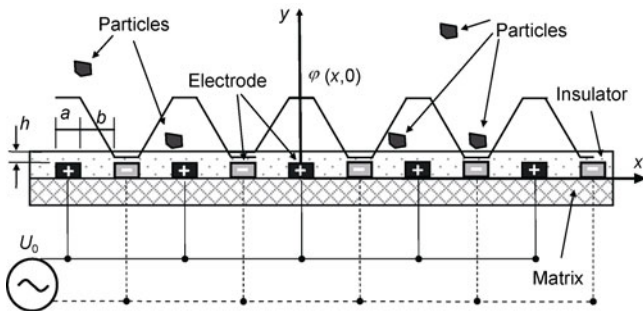
Figure 2 Structural parameters and potential distribution along an electric curtain.

leaving from the curtain, the particle collisions will occur and should be considered in the simulation. The detailed method to account for these processes will be explained below.

1.1 Electric field generated by electric curtain

The potential on surface of parallel electrodes is expressed by [27–29]:

$$\Phi(x, y, t) = U_0 \varphi(x, y)\cos(\omega t), \tag{1}$$

where $\omega = 2\pi f$ is an angular frequency, and $\varphi(x, y)$ is the potential induced by a unit electrostatic voltage. The electric field is related to the potential by $E_{x,y} = -\partial\Phi / \partial(x, y)$. The static potential can be written as Fourier series:

$$\varphi(x, y) = \sum_{n=0}^{\infty} a_n \cos(n\alpha x)\exp(-n\alpha y), \tag{2}$$

where a_n is the coefficient of Fourier expansion, $\alpha = \pi/p$, and $p = a + b$ is the periodicity of the electrodes. We get $a_n = \left(\lambda/n^2\pi^2 b\right)\left[\cos(n\pi a/\lambda) - \cos(n\pi(a+2b)/\lambda)\right]$ and $a_0 = 0.5$, $\lambda = 2p$ is the wavelength [30]. Finally the electric field over the EC surface is determined as:

$$E_x = -\frac{\partial\Phi}{\partial x} = U_0 \cos(\omega t)\sum_{n=1}^{+\infty} a_n n\alpha \sin(n\alpha x)\exp(-n\alpha y), \tag{3}$$

$$E_y = U_0 \cos(\omega t)\sum_{n=1}^{+\infty} a_n n\alpha \cos(n\alpha x)\exp(-n\alpha y). \tag{4}$$

Figure 3 shows the total electric field distribution over the EC surface within one period. In the computation, the following parameters are used a=0.2 mm, p=0.6 mm, U_0= 1500 V. From Figure 3, the electric field reaches a maximum value in the vicinity of the electrode edge due to discontinuity of the potential, and it decays exponentially
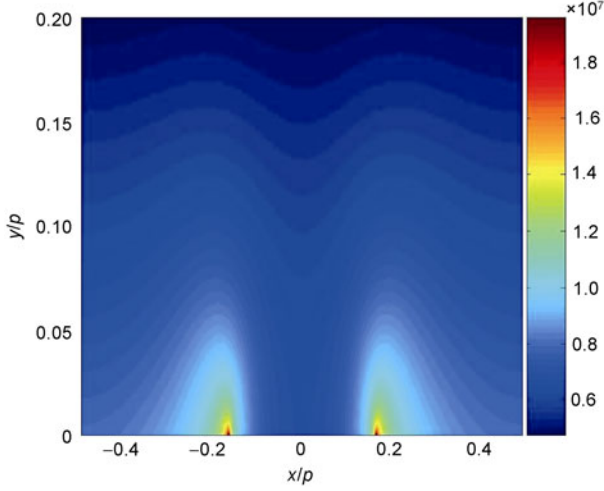
Figure 3 Distribution of electric field ($\sqrt{E_x^2 + E_y^2}$) over surface of EC within one period.

along the vertical direction.

1.2 Force exerting on the particle

When particles are leaving from surface of an EC, they will experience Coulomb force F_{Col} and dielectrophoresis force F_{Dep} [31,32], and on occasion will collide with each other. In the following simulation gravity is neglected and the particles are assumed to be spherical in shape and have the same size. The motion equation of a single particle can be written as [30]:

$$m\ddot{y} = F_{\text{Col},y} + F_{\text{Dep},y}, \tag{5}$$

$$m\ddot{x} = F_{\text{Col},x} + F_{\text{Dep},x}. \tag{6}$$

The Coulomb force F_{Col} and dielectrophoresis force F_{Dep} are calculated by $F_{\text{Col}}=QE$, $F_{\text{Dep}}=4\pi\varepsilon_0 r3kE\nabla E$, respectively, where Q is the electric charge of the particle, $k=(\varepsilon_r - 1)/(\varepsilon_r + 2)$, and ε_r, ε_0 are the dielectric constants of the particle and vacuum, respectively.

When the particles rest on the surface of the EC in an initial state or they fall back after leaping up, the contact between the particle and the curtain surface will produce significant adhesion and friction. Thus the motion equation of a particle on an EC surface should be expressed by

$$m\ddot{y} = F_{\text{Col},y} + F_{\text{Dep},y} + F_{\text{VDF}}, \tag{7}$$

$$m\ddot{x} = F_{\text{Col},x} + F_{\text{Dep},x} - \mu m|\ddot{y}|, \tag{8}$$

where F_{VDF} is the adhesion force calculated from van der Waals' force between the particle and the curtain surface [16]:

$$F_{\text{VDW}} = \frac{Ar}{12s^2}, \tag{9}$$

where r is radius of the particle, A is the Hamaker's constant ranging from $1–15\times10^{-19}$ J, s is the minimum distance between atoms, assuming for a contact problem that $s = 4\times10^{-10}$ [16]. The friction coefficient in eq. (8) is assumed to be $\mu = 0.02$.

1.3 Numerical implementation

Considering the case where particles are randomly placed on the surface of the EC, then the electrodes are loaded with a voltage at set time and the particles are driven to fly into the up to the EC. Each particle has an actual position, velocity and acceleration, and it moves according to Coulomb force F_{Col} and dielectrophoresis force F_{Dep} until a collision takes place. The collision is assumed to occur during a time step determined by the event-driven method [26]. The program estimates the time step for each particle pair that is likely to collide according to its relative position and velocity:

$$t_{ij} = \frac{-\boldsymbol{x}_r \cdot \boldsymbol{v}_r - [(\boldsymbol{x}_r \cdot \boldsymbol{v}_r)^2 - \boldsymbol{v}_r \cdot \boldsymbol{v}_r(\boldsymbol{x}_r \cdot \boldsymbol{x}_r - \sigma_{ij}^2)]^{1/2}}{\boldsymbol{v}_r \cdot \boldsymbol{v}_r}. \tag{10}$$

In eq. (10), $\boldsymbol{x}_r = \boldsymbol{x}_j - \boldsymbol{x}_i$ and $\boldsymbol{v}_r = \boldsymbol{v}_j - \boldsymbol{v}_i$ are the relative position and velocity of the particle pair, and $\sigma_{ij} = r_j + r_i$, $i \neq j$. The program then chooses the minimum time ($\min(t_{ij})$) as the time step Δt for all the particles. It is understandable that next collision only take place after Δt from the current one and terminates at the time $t + \Delta t$. Within the time increment Δt, each particle is considered to move with a constant velocity, thus at the end of the time increment, the particle moves to a new position of

$$\boldsymbol{x}_i(t + \Delta t) = \boldsymbol{x}_i(t) + \boldsymbol{v}_i(t)\Delta t. \tag{11}$$

Although the velocity $\boldsymbol{v}_i$ of the particle i is assumed to be constant during the time interval Δt, however, the forces (Coulomb force and Dielectrophoresis force) on the particle will lead its velocity at the time t to $t + \Delta t$ as:

$$\boldsymbol{v}_i(t + \Delta t) = \boldsymbol{v}_i(t) + \boldsymbol{a}_i(t)\Delta t, \tag{12}$$

where $\boldsymbol{a}_i$ is the acceleration of the particle i. Assuming elastic collisions among particles, when a particles α collides with a particle β, their velocities after the collision can be calculated by [26]

$$\boldsymbol{v}_\alpha = \boldsymbol{v}_{\alpha,0} + \left[\frac{2m_\beta}{m_\alpha + m_\beta}\frac{\boldsymbol{x}\boldsymbol{x}_{r,0} \cdot \boldsymbol{v}_{r,0}}{\sigma_{\alpha\beta}^2}\right]\boldsymbol{x}_{r,0}, \tag{13}$$

$$\boldsymbol{v}_\beta = \boldsymbol{v}_{\beta,0} + \left[\frac{2m_\alpha}{m_\alpha + m_\beta}\frac{\boldsymbol{x}_{r,0} \cdot \boldsymbol{v}_{r,0}}{\sigma_{\alpha\beta}^2}\right]\boldsymbol{x}_{r,0}, \tag{14}$$

where m_α and m_β are the masses of the particles α and β,

respectively. The above equations describe the collision process during $t + \Delta t$. Therefore the velocities are changed from $\boldsymbol{\upsilon}_{\alpha,0}$ and $\boldsymbol{\upsilon}_{\beta,0}$ to $\boldsymbol{\upsilon}_{\alpha}$ and $\boldsymbol{\upsilon}_{\beta}$ after the collision.

Immediately after the collision at the moment $t + \Delta t$, the forces acting on the particle are updated with a new position:

$$\boldsymbol{F}_{\text{Dep}}(t+\Delta t) = 4\pi\varepsilon_0 r^3 k \nabla \boldsymbol{E}_i^2 ((t+\Delta t), \boldsymbol{x}_i(t+\Delta t)), \quad (15)$$

$$\boldsymbol{F}_{\text{Col}}(t+\Delta t) = Q\boldsymbol{E}((t+\Delta t), \boldsymbol{x}_i(t+\Delta t)), \quad (16)$$

The acceleration is updated according to eqs. 5 and 6 (or 7 and 8). When the number of particles is small, only few collisions take place, the program executes quickly. As the number of particles increase, a large number of collisions will take places during in one time step Δt, the program is required to repeatedly recalculate the relative positions and velocities of all the particles.

2　Mechanism of particle leaping process

Let us examine particle motion driven by an electric curtain. We will first analyze leaping trajectory of a particle located at different initial positions on the surface of an EC and study influence of electric charges and then we will examine particle leaping process during a loading period. Different modes during the particle leaping process will be identified.

2.1　Influence of charge on particle trajectory at different initial positions

Electric charges are induced either by photoelectric charging or by particle collisions, the charge distribution being random among the particles [5,33]. From eqs. (5) and (7), it is seen that the electric charge plays a crucial role in particle motion. Particles with high electric charge more readily to leap away from surface of curtain [34]. Figures 4(a) and (b)

show the simulation on trajectory of a particle with $Q = Q_0$ and with $Q = 10Q_0$ located at different initial positions on surface of the EC, and $Q_0 = 3.64 \cdot 10^{-15} \text{C}$, taken from the value measured experimentally by Kawamoto [35]. The particle radius is $r = 10 \ \mu\text{m}$ [36], and the density is 2.9 g/cm³ [1], the frequency $f = 50$ Hz, while other parameters are the same as those in Figure 3. The particle is initially placed at different positions on the surface of the EC within a single period, and then its trajectory is calculated during loading. As shown by Figure 4(a), the low charged particle can only leap away from the EC surface when they are initially placed at the positions labeled by 1, 2 and 3, which are in proximity to the electrode. When placed at the locations of 4–11, that is, near the edge and the gap of the electrodes, the low charged particle can only roll along the surface of the EC. However, a highly charged particle can leap away directly from the EC surface at almost any initial positions, except in the middle of the gap between the electrodes, as shown in Figure 4(b).

Usually, the particles with high electrostatic charges are few [33], therefore we will focus on the movement of particles with a low electric charge, particularly for particles initially located at the unfavourable positions such as 4–11, shown in Figure 4(a).

2.2　Intermittent burst during particle leaping process

Five hundred particles were randomly scattered on the surface of the curtain and spanned over 18 electrodes. The size and density of the particles were the same as used in the previous calculation, the electrostatic charge of the particles were assumed to be $\pm Q_0$ with a sign randomly assigned, so that the total net charge of all particles is zero. The voltage, frequency and structural parameter of the EC were also the same as those in Figure 4. Figure 5 shows the simulated particle leaping process after the curtain is energized. The electrodes with high or low potentials are marked by red and blue, respectively, as well as the particles with positive
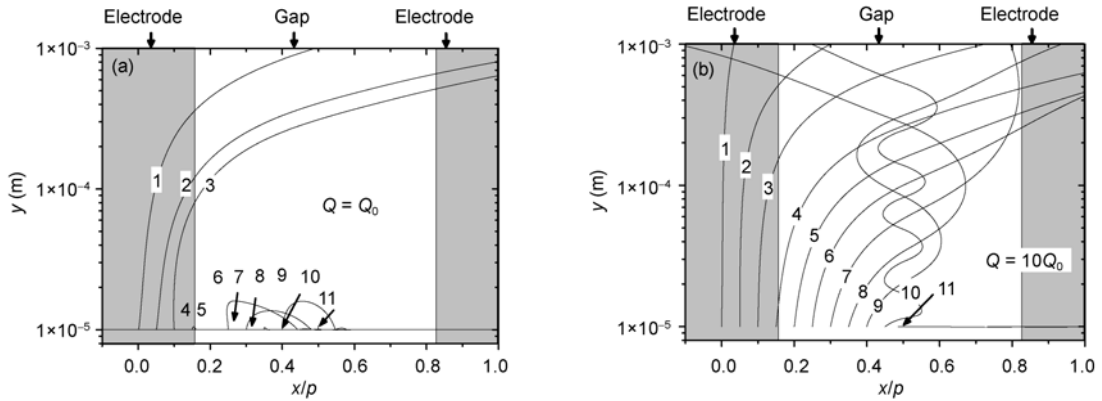
Figure 4　Trajectories of a low (a) or high (b) charged particle at different initial positions along EC surface.
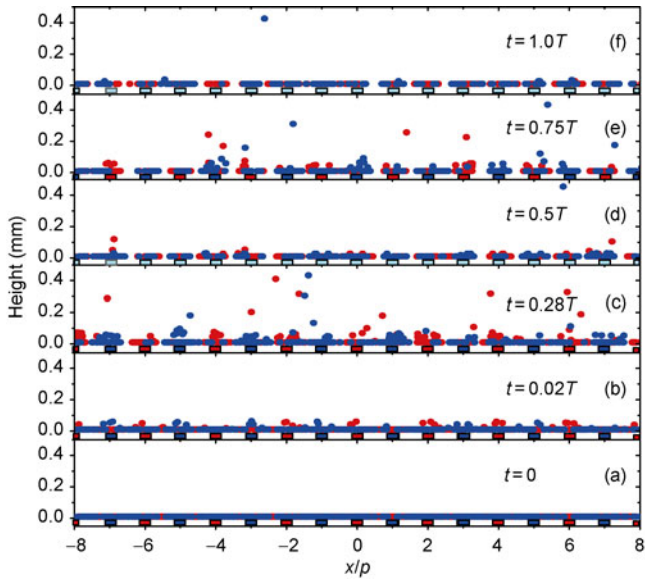
Figure 5 Particle motion pattern during a period of loading.

and negative electric charges. According to eqs. (3) and (4), there is no voltage potential at $t \approx 0.01s$ (0.5T) and $t \approx 0.02s$ (1.0T), so all electrodes are given as pale blue.

It is seen from Figure 5(b) that short after the EC was energized, the positive and negative charged particles leap up from the top of the electrodes. At the loading time 0.28T, the particle leaping process reaches a climax with a large

number of the particles starting to escape from the surface, as shown by Figure 5(c). At the moment 0.5T, the potential and electric field are nearly zero, with few particles leaping up. In Figure 5(d), we also realize that due to the flying of particles, several gaps among the particles are formed. Interestingly, the gaps are formed between the electrodes and not on the top of the electrodes where the particles leaped away. At time 3/4T, the potential is switched on again and a similar phenomenon as in Figure 5(c) is observed. At the end of one period (1.0T), there are only few particles that can leap up on the EC surface, as shown in Figure 5(f).

From Figure 5, we find that particles leap away from the top of the electrode with a burst period 0.5T in according to the variation of the electric field. The intermittent burst nature and the particle leaping positions during particle leaping process are also confirmed by a high speed camera observation, as shown in Figure 6. In the experiment, a pile of glass particles of radius 40–80 μm is placed on an EC surface (the size of the particle is larger than that used in the simulation in order to make the image more clear). The structural and electrical parameters of the EC are the same as those used in the above simulation. After loading at the time $t \approx 0.005s$ (0.25T), we observe that a few particles start to leap up from the pile (Figure 6(a)), at the time $t \approx 0.01s$ (0.5T) and a halt of particle ejection is observed (Figure 6(b)). At time $t \approx 0.015s$ (0.75T), many particle ejecting can be observed and again at $t \approx 0.02s$ (1.0T), the dust pile ex-
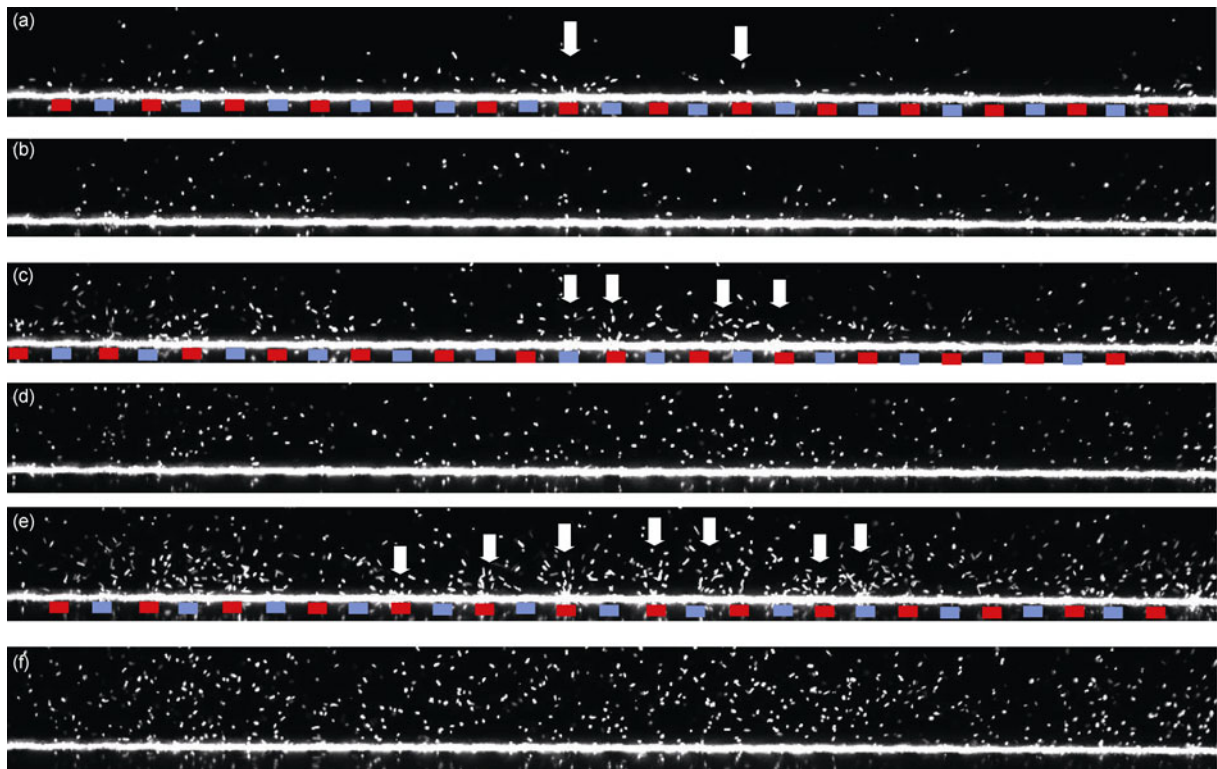
Figure 6 The intermittent burst during particle leaping process on an EC by high speed camera observation. (a) 0.005 s; (b) 0.010 s; (c) 0.015 s; (d) 0.020 s; (e) 0.025 s; (f) 0.030 s;

periences a recess. The experimental observation is in good agreement with the numerical simulation particularly on the positions of particle when starting to leap up and the burst interval of particle leaping process. A marked difference between the simulation and experiment is also observed. The number of particle leaping away from the EC surface at $t = 0.25T$ and $t = 0.75T$ decreases, as shown in Figure 5, while there is an increasing number of particle leaping spots at $t = 0.25T$ and $t = 0.75T$ in the experiment. This is due to the fact that, in simulation, the particles are considered as initially charged. However in the experiment, the particles possess no initial charges and they acquire growing tribo-charges during collision or rolling processes. Thus there are only few particles that start to leap up at the commencement of loading, e.g. $t = 0.25T$, since the particles have not accumulated enough electric charge.

2.3 Modes of particle leaping process and physical interpretation

The escaping mechanism of particles from an EC surface is usually attributed to two modes [34,37,38], that is. the hopping mode where the particles with high energy fly away directly from the EC surface without falling back, and the surfing mode where particles with low vertical velocity bounce up and down several times on the EC surface. To analyze the mechanism of these two modes, the time and location of each particle when it begins to leap away from the EC surface are examined. The reputed leap away here is defined as a state of a particle when it reaches a height as twice as its radius above the EC surface and it has a positive vertical velocity. This height is empirically chosen, we indeed find the number of particles crossing a typical height is changed according to the chosen height value, however, when this value is larger than $2r$, the number of particles crossing that height becomes stable. In this state, the particle can be rid of surface adhesion, and is less likely to be pulled back to the EC surface again. The computed leaping time and location are normalized by the loading period

T and the curtain space p. When the leaping position and time exceed the one period (space p or time T), we define the following parameters:

$$x'_{\text{Leap}} = -0.5p + \text{mod}(x_{\text{Leap}} + 0.5p, p) \cdot p, \qquad (17)$$

$$t'_{\text{Leap}} = \text{mod}(t_{\text{Leap}}, T), \qquad (18)$$

thus the leaping time and position for a particle in any moment and at any position can always be equivalently represented by a point within the time interval 0–T, the space range $-0.5p$–$0.5p$, which can be termed as a phase. The function mod is defined such that $\text{mod}(0.7p, p) = \text{mod}(1.7p, p) = 0.7p$. We consider the example as given in sect. 2.2 where the phases of five hundred particles are shown in Figure 7(a) by dots.

From Figure 7(a), we can note that the leaping phases primarily concentrate around four domains, that is. at $0.28T$ and $0.78T$ near both edges of the electrodes, as marked by the circles in the Figure 7(a). Again, the time interval between two burst phases is $0.5T$. As discussed above, the preferred positions for particles leaping up are the edges of the electrodes. Only few particles can leap up directly at the gap of the electrodes. This suggests that there must be a particle transportation process along the EC surface, which transports the particles initially located at the gaps of the electrodes toward their edges, and then the particles gather sufficient force and leap away from the surface.

The leaping velocities of the particles are also calculated to analyze the modes of the particle motion. Figure 7(b) shows the ratio of vertical to horizontal velocities as function of the leaping positions along the EC surface at the moment where a particle start to leap away. The ratios are calculated by averaging the velocities of all particles leaping at the same location. It is seen that particles leaping from the top of the electrode possess a large vertical velocity, and can be attributed to the hopping mode, while particles leaping from the edge of the electrode have a small vertical velocity, thus can be considered to have the surfing mode.
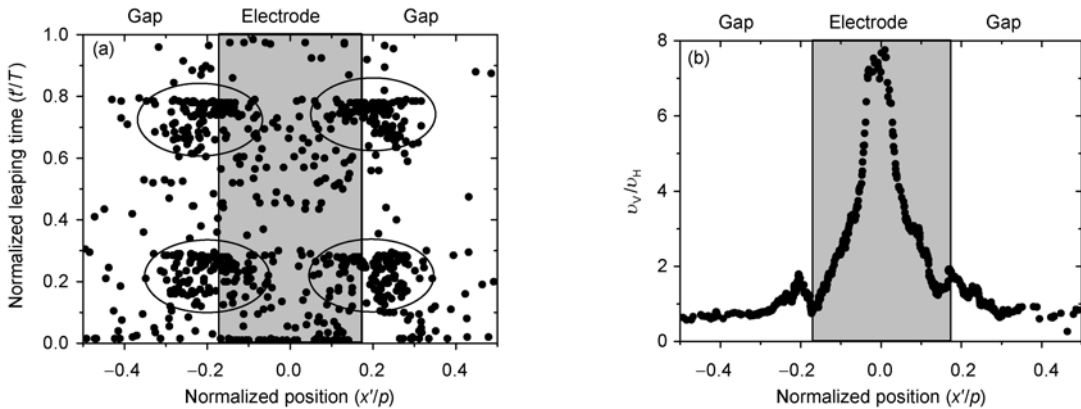
Figure 7 (a) Normalized leaping times and positions; (b) ratio of vertical to horizontal velocities as function of normalized leaping positions.

Determining from the number of points showing in Figure 7(b), we also find that the majority of the particles assume the surfing mode. Few particles, initially on the top of the electrode, assume the hopping mode.

From the above simulation, the scenario of particle motion on an EC surface can be summarized as the following. Initially the, particles located on the tops of the electrodes first start to leap away from the EC surface in the hopping mode. Then the particles initially located at the gaps of the electrodes move horizontally toward the edges of the electrodes, are energized and leap away. The horizontal motion enables these particles to have a comparably large transverse velocity, thus these particles mainly leap away in the surfing mode. During the transverse movement, the particles keep in contact with the EC surface, thus the friction of the particles on the EC surface will affect removal efficiency.

One notable effect of the friction is that it prevents the particles from reaching proper leaping phases. Figure 8 shows the particle patterns on the EC surface at 0, 0.1, 0.5, 1.0 and 1.5 s after energizing. As the particles leap up and fly away, the number of particles remained on the surface of the EC gradually reduces. After driven by the high electric field at 0.5s, the majority of the particles have been removed with only a small part of particles remain at the vicinities of the electrode edges or at the middle position on top of the electrodes. These remained particles are difficult to be repelled off even with further loading. This may explain why some residues consistently remain during dust removal in the experiment.
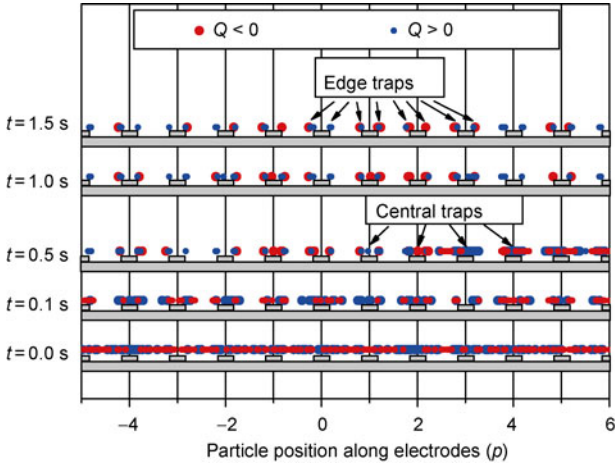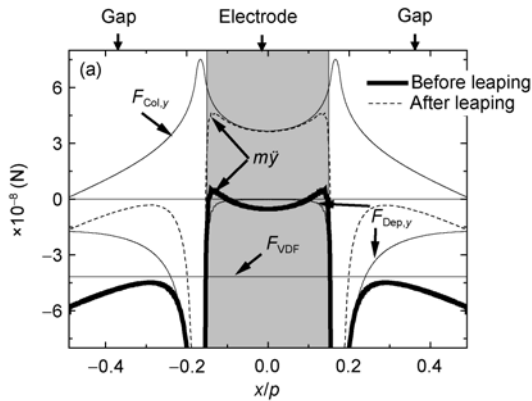
The particle leaping process, leaping mode and particle trap on an EC surface can be well explained by the forces exerted on the particle. Figure 9 shows the variation of vertical forces and horizontal forces loaded on a particle with a charge Q_0 when the particle is located at different positions along the EC surface. The radius and density of the particle, structural and electrical parameters of the EC remain the same as previously used. The total vertical and horizontal forces experienced by a particle flying over or contacting to the EC surface are calculated from eqs. (5) to (8), respectively.

Figure 9(a) explains the reason why the majority of the particles start to leap away at the vicinity of the edge of the electrode. From the bold line, we note that the resistant forces (dielectrophoresis force, adhesion force F_{VDF}) lead to a resultant force ($m\ddot{y}$, see eq. (7)) that can only be positive near the edge of the electrode when the particle is contacted to the EC surface. Thus particles initially located in the gap can only leap away after moving from their initial positions to the edges of the electrodes by the horizontal forces.

The bold lines in Figure 9 also show which mode a particle will take when it starts to leap up. For the particles on the top of the electrode, they will experience a large vertical force and a small horizontal force, thus they can acquire comparably a large vertical velocity, therefore assume the hopping mode. For particles at the edge of the electrode, the exerted horizontal force reaches a maximum value, thus they will acquire a large transverse velocity, and assume the surfing mode.

The particle traps on the EC surface are also explained by Figure 9(b). According to eq. (8), when the total horizontal force shown by the bold line in Figure 9(b) becomes

Figure 8 The positions of particles remaining on the electric curtain surface at different times.
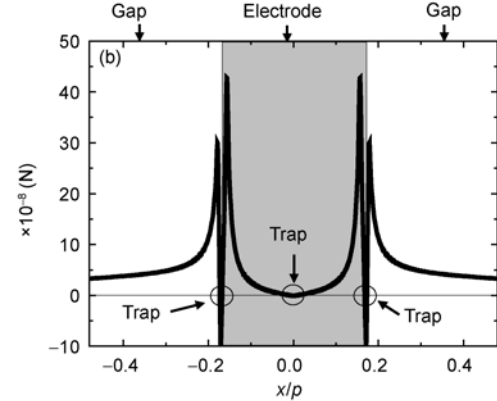
Figure 9 The vertical (a) and horizontal (b) forces acting on a particle at different positions.

zero or negative, it can be considered that the friction force is larger than the driving force. Therefore the particles at such locations will not move transversely. The calculated locations where the total horizontal forces become zero or negative are marked by circles in Figure 9(b). One could readily see that the edge and central position of the electrode are indeed the positions of particle traps, as already demonstrated in Figure 8.

3   Summary and conclusion

Dust poses severe problems in lunar or Mars surface explorations. The electric curtain technique is considered as a promising approach to alleviate dust problem. Based on particle dynamic simulation and experimental observation, the paper presents a detailed analysis on the mechanism of dust removal by an electric curtain. The charged particles are found to leap away from the tops of the electrodes with an intermittent burst of a half period. It is also shown that particles located in the gaps of the electrodes first move transversely toward the edges of the electrodes and then begin to leap up. A part of the particles can be trapped at the edges of the electrodes and this will affect the dust removal efficiency of the electric curtain technique.

1   Heiken G, Vaniman D, French B M, et al. Lunar Sourcebook: A User's Guide to the Moon. Cambridge: Cambridge University Press, 1991

2   Ouyang Z Y. Introduction to Lunar Science. Beijing: China Astronautics, 2005

3   McCoy J, Criswell D. Evidence for a high altitude distribution of lunar dust. In: Proc. 5th Lunar Science Conference, Houston, Tex, 1974. 2991–3005

4   Rennilson J, Criswell D. Surveyor observations of lunar horizon glow. Moon, 1974(2), 10: 121–142

5   Walton O R. Adhesion of Lunar Dust. Technical Report, NASA/CR-2007-214685, 2007

6   Carroll W F, Blair P M. Spacecraft changes: Lunar dust and radiation darkening of Surveyor 3 surfaces. In: Analysis of Surveyor 3 Material and Photographs. Technical Report, N72_26731, 1971. 23

7   Gold T, Williams G J. Electrostatic transportation of dust on the moon, photon and particle interactions with surfaces in space. Astrophys Space Sci, 1973, 37: 557–660

8   Bates J R, Fang P H. Results of solar cell performance on lunar base derived from Apollo missions. Solar Energy Mater Solar Cells, 1992, 26: 79–84

9   Wood K. Design of Equipment for Lunar Dust Removal. Technical Report, NASA2CR-190014, 1991

10   Tatom F B, Srepel V, Johnson R D, et al. Lunar Dust Degradation Effects and Removal/Prevention Concepts. Northrop/Huntsville Technical Report, TR-792-7-207A , 1967

11   Sims R A, Biris A S, Wilson J D, et al. Development of a transparent self-cleaning dust shield for solar panels. In: Proceedings of the First Joint Meeting IEEE-IAS and Electrostatics Society of America, Pasadena, California, 2000. 814–821

12   Calle C I, Buhler C R, Mantovani J G, et al. Electrodynamic shield to remove dust from solar panels on Mars. In: Proceedings of the 41st Space Congress, Cape Canaveral, 2004

13   Calle C I, Mazumder M K, Immer C D, et al. Controlled particle removal from surfaces by electrodynamic methods for terrestrial, lunar and martian environmental conditions. J Phys, 2008, 142: 012073

14   Masuda S. Advances in Static Electricity. Brussels: Auxilia, 1970, 2: 398–414

15   Kawamoto H. Electrostatic and electromagnetic cleaning of lunar dust adhered to spacesuits. In: Annual Meeting of LEAG, Houston, Texas, 2009

16   Atten P, Pang H L, Reboud J. Study of dust removal by standing wave electric curtain for application to solar cells on Mars. IEEE IAS, 2005, 1: 334–340

17   Mazumder M K, Sims R A, Wilson J D. Transparent Self-Cleaning Dust Shield. U.S. Pat. Appl. Publ., 2004, 20040055632

18   Moesner F M, Higuchi T. Traveling electric field conveyor for contactless manipulation of microparts. IEEE Ind Appl Soc Annu Meeting, 1997, 3: 2004–2011

19   Cao H X, Ruan P, Li T, et al. Summary of lunar dust removal methods for optical system (in Chinese). Sci Tech Eng, 2007, 7: 1671–1676

20   Shi X B, Li Y Z, Huang Y, et al. Study on the simulation strategy of lunar dust/regolith environment effects. Chin J Space Sci, 2007, 27(1): 66–71

21   Yuan Y F, Liu M, Bai X C. Research of electrode screen as dust mitigation technology (in Chinese). Spacecraft Eng, 2010, 19: 89–94

22   Machowski W, Balachandran W. Electrodynamic control and separation of charged particles using travelling wave field technique. J Electrostatics , 1997, 41: 325–330

23   Johnson C E, Srirama P K, Sharma R, et al. Effect of particle size distribution on the performance of electrodynamic screens. IEEE IAS, 2005 1: 341–345

24   Calle C I, Buthler C R. Electrodynamic dust shield for solar panels on mars. Lunar and Planetary Science XXXV, 2004

25   Biris A S, Saini D. Electrodynamics removal of contaminant particles and its application. IEEE IAS, 2004, 2: 1283–1286

26   Duff N, Lacks D J. Particle dynamics simulations of triboelectric charging in granular insulator systems. J Electrostatics, 2008, 66: 51–57

27   Mazumder M K, Sharma R, Biris A S, et al. Self-cleaning transparent dust shields for protecting solar panels and other devices. Particul Sci Technol, 2007, 25(1): 5–20

28   Masuda S, Washizu M, Iwadare M. Separation of small particles suspended in liquid by nonuniform traveling field. IEEE Trans, 1987, 23(3): 474–480

29   Masuda S, Tsutomu K. Approximate methods for calculating a non-uniform travelling field. J Electrostatics, 1975, 1: 351–370

30   Sun Q X, Yang N N, Xiao Z K, et al. Experimental study on dust removal efficiency of standing wave electric curtain. Spacecraft Eng, In Press

31   Jones T B. Electromechanics of Particles. Cambridge: Cambridge University Press, 1995

32   Landau L D, Lifshitz E M. Electrodynamics of Continuous Media. Oxford: Butterworth-Heinemann Ltd, 1984

33   Sickafoose A A, Colwell J E, Horányi M, et al. Experimental investigations on photoelectric and triboelectric charging of dust. J Geophys Res, 2011, 106(5): 8343–8356

34   Liu G, Marshall J S. Particle transport by standing waves on an electric curtain. J Electrostatics, 2010, 68(4): 289–298

35   Kawamoto H, Seki K, Kuromiya N. Mechanism of travelling-wave transport of particles. J Phys D-Appl Phys, 2006 39(6): 1249–1256

36   Park J, Liu Y, Kihm K D, et al. Characterization of lunar dust for toxicological studies I: particle size distribution. J Aerospace Eng, 2008, 21(4): 266–271

37   Dudzicz Z. The path of oscillation of dust particles in the field of the electric curtain of the plane type supplied with AC voltage. J Electrostatics, 1989, 23: 207–214

38   Liu G Q, Marshall J S. Effect of particle adhesion and interactions on motion by traveling waves on an electric curtain. J Electrostatics, 2010, 68(2): 179–189